Towards Large Language Models with Self-Consistent Natural Language Explanations

Sahar Admoni¹, Ofra Amir¹, Assaf Hallak², Yftah Ziser²

¹Technion – Israel Institute of Technology ²Nvidia Research

saharad@campus.technion.ac.il, oamir@technion.ac.il, {ahallak,yziser}@nvidia.com

Abstract

Large language models (LLMs) seem to offer an easy path to interpretability: just ask them to explain their decisions. Yet, studies show that these post-hoc explanations often misrepresent the true decision process, as revealed by mismatches in feature importance. Despite growing evidence of this inconsistency, no systematic solutions have emerged—partly due to the high cost of estimating feature importance, which limits evaluations to small datasets. To address this, we introduce the Post-hoc Self-Consistency Bank (PSCB)—a large-scale benchmark of decisions spanning diverse tasks and models, each paired with LLMgenerated explanations and corresponding feature importance scores. Analysis of PSCB reveals that self-consistency scores barely differ between correct and incorrect predictions. We also show that the standard metric fails to meaningfully distinguish between explanations. To overcome this limitation, we propose an alternative metric that more effectively captures variation in explanation quality. We use it to finetune LLMs via Direct Preference Optimization (DPO), leading to significantly better alignment between explanations and decision-relevant features—even under domain shift. Our findings point to a scalable path toward more trustworthy, self-consistent LLMs.¹

1 Introduction

As Large language models (LLMs) are increasingly embedded in user-facing and decision-support systems, their outputs—and especially the explanations accompanying them—are often trusted by end users, even when independent verification of correctness or reasoning is impractical (Sun et al., 2024). To foster trust, LLMs are often prompted to provide natural language explanations (NLEs) to articulate their reasoning (Quan et al., 2024).

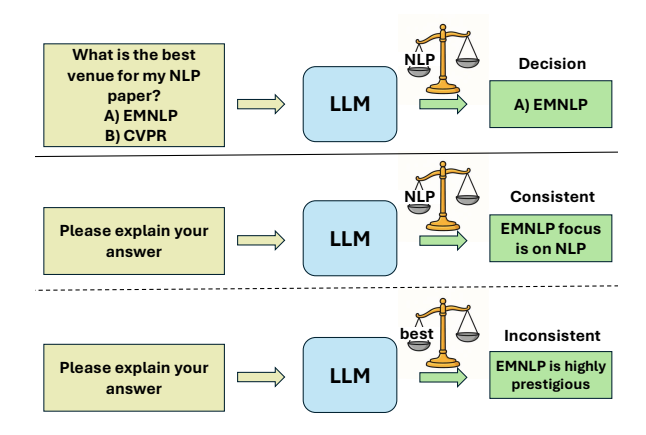


Figure 1: Illustration of explanation consistency using feature importance. **Top:** The LLM generates an answer where the word *NLP* in the prompt has high feature importance. **Middle:** A consistent explanation where *NLP* in the prompt also has high feature importance. **Bottom:** An inconsistent explanation, where the word *best* in the prompt has high feature importance instead, misaligned with the model's actual decision.

However, these explanations frequently fail to reflect the model's inner decision process, a shortcoming known as a lack of faithfulness (Lyu et al., 2022). A related concept, self-consistency, measures the degree of alignment between the model's decisions and the explanation, particularly in terms of feature importance. While self-consistency is not equivalent to faithfulness, it is widely viewed as a necessary prerequisite (Parcalabescu and Frank, 2023). Inconsistent explanations signal misalignment between reasoning and justifications, undermining trust in high-stakes domains like healthcare, law, or education. LLMs typically produce explanations through: (i) chain-of-thought reasoning, where the explanation is generated as part of the model's reasoning process (Wei et al., 2022), and (ii) justifications generated after decisions (Wiegreffe et al., 2020) (Figure 1). We focus on the latter. Prior work has proposed methods to evaluate selfconsistency in these settings (Turpin et al., 2023;

¹Code and data will be released upon acceptance.

Lanham et al., 2023; Atanasova et al., 2023; Wiegreffe et al., 2020), but improving self-consistency remains an open challenge.

In this work, we take a step forward by introducing new benchmarks, metrics, and methods to enhance explanation consistency. We introduce the post-hoc self-consistency bank (PSCB) to systematically evaluate and improve explanation consistency across multiple LLMs and datasets. We compare two complementary consistency metrics and apply Direct Preference Optimization (DPO) (Rafailov et al., 2023) to enhance consistency. Our contributions include:

- Post-hoc Self-Consistency Bank (PSCB): We introduce PSCB, a large-scale benchmark for evaluating natural language explanation (NLE) self-consistency in LLMs, consisting of over 23,000 model decisions, each annotated with an attribution vector and paired with five explanations, each accompanied by its own attribution vector—totaling over 116,000 explanation instances—collected across four multiple-choice QA datasets and two instruction-tuned LLMs.
- Empirical analysis of self-consistency: We conduct the first large-scale analysis of attribution-based self-consistency in LLMs and find that self-consistency is unaffected by whether the model's answer is correct. We showcase the effectiveness of Spearman rank correlation as an alignment metric, highlighting its strong discriminative ability to capture quality differences across candidate explanations.
- Improving self-consistency via preference supervision: We demonstrate that attribution-based preference data—automatically derived from our PSCB benchmark—can be used to fine-tune LLMs with Direct Preference Optimization (DPO), to improve self-consistency, both in-domain and with robust cross-domain generalization.

2 Background and Related Work

2.1 Feature Attribution Methods

Feature attribution methods estimate the contribution of input components (e.g., tokens) or internal elements (e.g., attention heads) and are central to interpreting model predictions (Zhao et al., 2023). *Attention-based* methods are appealing due to their simplicity and low cost, but are widely criticized as unreliable indicators of importance (Jain and Wallace, 2019; Serrano and

Smith, 2019; Wiegreffe and Pinter, 2019). More robust alternatives include gradient-based methods, which use backpropagation to assign importance scores—e.g., Integrated Gradients (Sundararajan et al., 2017) and LRP (Bach et al., 2015; Montavon et al., 2019)—and perturbation-based methods, which modify inputs and observe output changes. Notable examples of the latter include input masking (Petsiuk et al., 2018), Shapley value estimation via SHAP (Lundberg and Lee, 2017), and surrogate model fitting as used in LIME (Ribeiro et al., 2016). While SHAP offers strong theoretical guarantees, it is computationally expensive, especially for large models. LIME, in contrast, provides a practical middle ground—offering informative explanations with much lower computational cost.

2.2 NLE Self-Consistency

A faithful natural language explanation (NLE) reflects the reasoning behind a model's prediction, not just a plausible-sounding justification (Jacovi and Goldberg, 2020). However, LLMs often generate fluent explanations that diverge from their actual decision process (Narang et al., 2020; Turpin et al., 2023), prompting a shift toward evaluating self-consistency—the extent to which explanations rely on the same input features or reasoning patterns as the predictions. Self-consistency has emerged as a practical proxy for faithfulness, supported by diverse evaluation strategies. Perturbation-based methods test explanation robustness through counterfactual edits, noise injection, misleading feature bias, or corrupted chain-ofthought reasoning (Atanasova et al., 2023; Wiegreffe et al., 2020; Turpin et al., 2023; Lanham et al., 2023). Attribution-based approaches offer a more direct assessment by comparing feature importance vectors. For instance, CC-SHAP (Parcalabescu and Frank, 2023) evaluates consistency via Shapley value alignment between predictions and explanations. While precise and model-agnostic, such methods have been limited to small-scale datasets, raising questions about their scalability.

3 Post-hoc Self-Consistency Bank

This section introduces the *Post-hoc Self-Consistency Bank*. We describe the key components needed to construct each dataset: a base question-answering dataset, a target LLM, and a self-consistency metric. We then outline our design choices for building the full bank and conclude

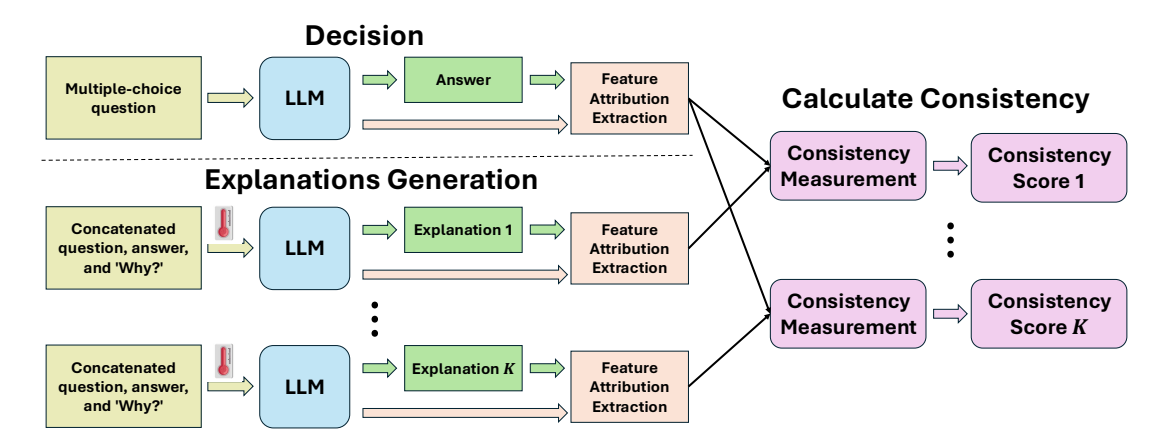


Figure 2: Overview of the PSCB pipeline. Given a multiple-choice QA instance, the LLM generates an answer and associated attribution scores over the input. It is then prompted to produce K diverse explanations (via temperature sampling) conditioned on the question and answer. Attributions are recorded for each explanation, and self-consistency scores are computed between decision and explanation attributions.

with key statistics and findings. Our pipeline (Figure 2) is inspired by CC-SHAP (Parcalabescu and Frank, 2023) and generalizes to diverse feature attribution methods and alignment metrics.

3.1 Sequence Feature Attribution

To analyze which input tokens influence a model's generation behavior, we compute token-level attribution scores for sequence outputs. These scores identify the features most responsible for the model's confidence in its predictions.

Input and Output Definition. Let the input be a token sequence $\mathbf{x} = [x_1, x_2, \dots, x_m]$ of length m, and the output be a generated sequence $\mathbf{y} = [y_1, y_2, \dots, y_n]$ of length n. The model generates \mathbf{y} autoregressively, producing a logit vector $\ell_t \in \mathbb{R}^V$ over the vocabulary V at each decoding step t.

Output Scoring. We define a scalar confidence score for the full sequence as the sum of log-probabilities: $\operatorname{score}(\mathbf{x},\mathbf{y}) = \sum_{t=1}^n \log P(y_t)$, where $\log P(y_t) = \log \left(\frac{\exp(\ell_t[y_t])}{\sum_{v \in V} \exp(\ell_t[v])}\right)$. This scalar represents the target quantity for attribution: how much each token in \mathbf{x} contributes to the overall model confidence in generating \mathbf{y} .

Attribution Computation. We compute a token-level attribution vector over the input:

$$\phi^{(\mathbf{y})} = [\phi_1^{(\mathbf{y})}, \phi_2^{(\mathbf{y})}, \dots, \phi_m^{(\mathbf{y})}],$$

where $\phi_i^{(y)}$ quantifies the contribution of token x_i to the model's confidence in generating y. The attribution method—whether gradient-based, perturbation-based, or sampling-based—determines how $\phi^{(y)}$ is computed. In our framework, this process is method-agnostic; specific techniques are described in Section 3.4.

Skip Token Filtering. To avoid noise from irrelevant symbols, we define a set of *skip tokens* $S \subseteq V$ (e.g., punctuation, special formatting). Tokens $x_i \in S$ are excluded from the attribution process by holding them fixed during perturbation or masking steps. This focuses attribution on semantically meaningful inputs.

3.2 Measuring Self-Consistency

To evaluate whether a model's explanation reflects the reasoning behind its decision, we assess the alignment between two attribution vectors derived from the same input x:

- y_{dec} : the model's predicted answer or decision.
- y_{exp}: a post-hoc natural language explanation generated by conditioning on both x and y_{dec}.

Let $\phi^{(y_{\rm dec})}$ and $\phi^{(y_{\rm exp})}$ denote the attribution vectors over ${\bf x}$ for the decision and the explanation, respectively. We quantify the self-consistency using a similarity metric that measures alignment between the two attribution vectors ${\cal M}\left(\phi^{(y_{\rm dec})},\phi^{(y_{\rm exp})}\right)$: ${\mathbb R}^m\times{\mathbb R}^m\to{\mathbb R}$. The choice of ${\cal M}$ determines the aspect of alignment being evaluated (e.g., magnitude, rank, overlap), and is discussed in detail in the following subsections.

3.3 Constructing Attribution-Based Preference Data

To support the evaluation and improvement of self-consistency in natural language explanations (NLEs), we construct a dataset where each instance contains both model outputs (decisions and explanations) and their corresponding input attribution vectors. This structure enables fine-grained, token-level comparisons between the model's decision rationale and its post-hoc justifications.

Attribution-Enhanced Instances. Each instance is represented as a structured quintuple:

$$\left(\mathbf{x},\ \mathbf{y}_{\text{dec}},\ \left\{\mathbf{y}_{\text{exp}}^{(i)}\right\}_{i=1}^{k},\ \boldsymbol{\phi}^{(\mathbf{y}_{\text{dec}})},\ \left\{\boldsymbol{\phi}^{(\mathbf{y}_{\text{exp}}^{(i)})}\right\}_{i=1}^{k}\right),$$

where \mathbf{x} is the original multiple-choice question, \mathbf{y}_{dec} is the model's predicted answer to \mathbf{x} , $\left\{\mathbf{y}_{\text{exp}}^{(i)}\right\}_{i=1}^k$ are k post-hoc explanations conditioned on both \mathbf{x} and \mathbf{y}_{dec} , $\phi^{(\mathbf{y}_{\text{dec}})}$ is the attribution vector over \mathbf{x} for the decision, and $\left\{\phi^{(\mathbf{y}_{\text{exp}}^{(i)})}\right\}_{i=1}^k$ are attribution vectors for the explanations. This format allows us to compare explanation alignment across multiple candidate justifications.

Output Generation. For each input \mathbf{x} , we prompt an instruction-tuned language model in a zero-shot setting to produce a decision \mathbf{y}_{dec} . We then sample k diverse post-hoc explanations $\mathbf{y}_{\text{exp}}^{(i)}$ conditioned on both \mathbf{x} and \mathbf{y}_{dec} . This setup yields multiple plausible explanations for the same decision, enabling relative alignment comparison.

Attribution Computation. We compute attribution vectors over the input \mathbf{x} for both the decision and each explanation, based on the log-likelihood of the generated output sequence. Our framework is method-agnostic and supports a range of feature attribution techniques, including gradient-based and perturbation-based methods. Formatting and special tokens are excluded from attribution to focus on semantically meaningful content.

Alignment-Based Labeling. We measure attribution alignment between each explanation and the decision using the metrics introduced in the previous subsection. Each explanation is scored based on its alignment with the decision, and we retain the highest- and lowest-scoring examples as $\mathbf{y}_{\text{exp}}^{\text{chosen}}$ and $\mathbf{y}_{\text{exp}}^{\text{rejected}}$, respectively. These ranked pairs form the basis for the preference optimization objective described in the next section.

3.4 Experimental Setup

Models. We evaluate two instruction-tuned language models from the LLaMA family: LLaMA-

	Metric		LLaMA3.1- 8B	LLaMA3.2- 3B
2	Acc.		71.11	65.85
ECQA (#10882)	CC-Cos	Worst	07.70	01.30
#1		Mean	08.18	01.65
A (4		Best	08.67	01.99
\mathcal{S}		Worst	05.07	09.75
<u> </u>	CC-Sp	Mean	18.47	22.28
		Best	31.76	34.64
5	Acc.		87.01	81.90
ARC-E (#5197)		Worst	13.31	05.32
#	CC-Cos	Mean	14.16	05.86
E .		Best	15.02	06.41
K		Worst	-01.06	07.26
⋖	CC-Sp	Mean	12.44	19.68
		Best	25.77	31.98
ARC-C (#2590)	Acc.		77.57	68.70
	CC-Cos	Worst	15.09	07.67
		Mean	16.07	08.29
		Best	17.08	08.93
	CC-Sp	Worst	-01.82	05.94
₹		Mean	11.48	18.44
		Best	24.73	30.89
(9	Acc.		83.39	75.48
277	CC-Cos	Worst	12.87	07.49
#		Mean	13.68	08.06
H-t		Best	14.52	08.64
C oda-H (#2776)		Worst	07.11	06.82
\circ	CC-Sp	Mean	19.97	19.39
		Best	32.66	31.95

Table 1: Evaluation results across tasks. Acc. = Accuracy; Cos = CC-LIME-Cos; Sp = CC-LIME-Sp; (x100).

3.1-8B-Instruct and LLaMA-3.2-3B-Instruct (Touvron et al., 2023). All models are used in a zeroshot setting. To ensure compatibility with generation and attribution scoring, we add a padding token.

Datasets. We evaluate four diverse multiple-choice question-answering (MCQA) datasets: ECQA (Aggarwal et al., 2021), ARC-Easy, ARC-Challenge (Clark et al., 2018), and CODAH (Chen et al., 2019). Each dataset contains 4–5 answer multiple-choice questions and is used to probe explanation consistency in different reasoning domains. We first preprocess each dataset into our unified attribution-enhanced format (Section 3.3) and then randomly split the resulting instances into the train (70%), validation (20%), and test (10%) sets using a fixed random seed. We use the training set to generate explanations and construct attribution-based preference pairs, the validation set for model selection, and the test set for final evaluation. For

each training instance, we sample k=5 candidate explanations.

Prompting and Generation. To elicit decisions, we use a minimal task instruction prompt (e.g., "Choose the best plausible answer:"), and then generate post-hoc natural language explanations by conditioning on both the question \mathbf{x} and the model's answer \mathbf{y}_{dec} . Explanations are generated using nucleus sampling with top-p = 0.9, temperature = 0.7, and a maximum output length of 400 tokens. Complete prompt templates are provided in Appendix A.

Feature Attribution. We use the LIME feature attribution method (Ribeiro et al., 2016), as implemented in Captum (Kokhlikyan et al., 2020), to compute input token attributions with respect to the log-likelihood of the generated output sequence. We use 500 perturbation samples per example and set the reference input to the padding token repeated across the input length. Punctuation and formatting tokens (e.g., special symbols) are excluded from attribution using a manually defined skip list (see Appendix C).

Consistency Metrics. We compare the feature attribution vectors using two complementary alignment metrics that capture different aspects of self-consistency. *Cosine Similarity* quantifies how well an explanation's attributions align with the decision's direction and strength. Higher values indicate greater overlap in both the identity and importance of input features. Similar cosine-based comparisons were used in CC-SHAP (Parcalabescu and Frank, 2023). *Spearman Rank Correlation* assesses consistency in feature prioritization while abstracting away from attribution magnitudes:

$$CC_{sp} = 1 - \frac{6\sum_{i=1}^{m} \left(r\left(\phi_{i}^{(\mathbf{y}_{dec})}\right) - r\left(\phi_{i}^{(\mathbf{y}_{exp})}\right)\right)^{2}}{m(m^{2} - 1)}.$$

Here, $\mathbf{r}(\cdot)$ assigns ordinal ranks to the attribution values, with rank 1 for the minimal score and m for the largest; ties are resolved using average rank. This metric captures how similarly the two outputs prioritize input features, abstracting away from exact attribution values.

Together, these metrics capture different aspects of alignment: cosine similarity measures directional agreement, while Spearman captures feature ranking. High scores indicate that explanations highlight features similar to those of the decision,

suggesting self-consistency; low scores imply divergent reasoning and reduced trust.

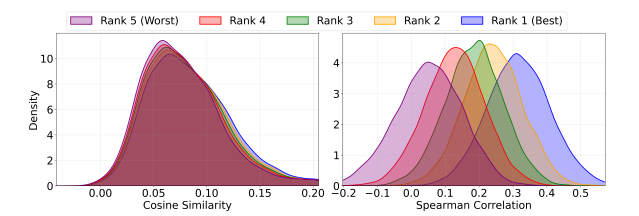


Figure 3: Smoothed distribution of self-consistency scores by explanation rank for the LLaMA3.1-8B model on ECQA. **Spearman correlation (right)** shows clear rank separation, reflecting strong sensitivity to explanation quality. **Cosine similarity (left)** shows substantial overlap across ranks, indicating weaker differentiation.

3.5 Key Findings and Insights

We evaluate attribution-based self-consistency across four MCQA datasets and two instruction-tuned language models, as shown in Table 1. We report decision accuracy for each model—dataset pair and compute self-consistency scores using five sampled explanations per input. Consistency is measured via cosine similarity (CC-LIME-COS) and Spearman rank correlation (CC-LIME-SP), reporting the *worst*, *mean*, and *best* alignment scores.

Explanation variability and metric differences.

We observe large gaps between the best and worst explanations per input. For instance, in ECQA with LLaMA3.1-8B, Spearman scores range from 5.07 to 31.76. Across settings, Spearman scores are generally higher than cosine scores, suggesting that models more consistently preserve feature ranking than exact attribution magnitudes. This greater variability makes Spearman particularly well-suited for identifying improvements, as it varies more significantly across explanations than cosine similarity, which tends to yield more compressed, lower values due to its sensitivity to attribution intensity. This variability confirms the need for a rankingbased evaluation and highlights the opportunity to identify highly self-consistent explanations from diverse generations (see Figure 3). Figure 4 illustrates that the large variance in Spearman correlation reflects meaningful semantic differences in explanation consistency.

Correctness and self-consistency. To assess whether explanation self-consistency correlates with model correctness, we compare alignment scores for correct and incorrect predictions (Table 2). While some models show marginally higher

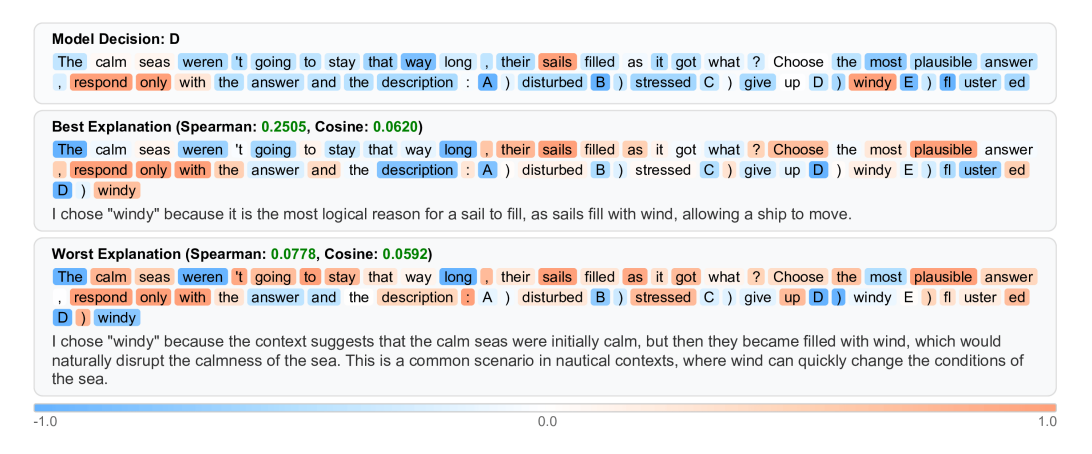


Figure 4: An example from the ECQA dataset shows attribution alignment for the LLaMA3.2-3B model's decision and its best (Sp=0.25) and worst (Sp=0.08) explanations. The model selects answer "D" ("windy"), with attribution heatmaps highlighting word-level influences (blue = negative, orange = positive). Key tokens like "sails" and "windy" drive the decision. The best explanation mirrors this focus, correctly reasoning that wind fills sails, while the worst shifts emphasis to "calm seas," misaligning with the core mechanism.

self-consistency when correct, the differences are small and inconsistent. For instance, in ECQA with LLaMA3.1-8B, Spearman is slightly higher when correct (0.186 vs. 0.182), whereas in ARC-Easy with LLaMA3.2-3B, it is slightly higher when incorrect. Overall, we find no clear or robust trend linking correctness to explanation alignment, indicating that self-consistency captures a property orthogonal to prediction accuracy.

	Model	CC-Cos (C / I / Δ)	CC-Sp (C / I / Δ)
ECQA	LLaMA3.1-8B	8.1 / 8.4 / -0.3	18.6 / 18.2 / +0.4
	LLaMA3.2-3B	1.6 / 1.7 / -0.1	22.3 / 22.3 / 0.0
ARC-E	LLaMA3.1-8B	14.1 / 14.8 / -0.7	12.4 / 13.0 / -0.6
	LLaMA3.2-3B	5.7 / 6.6 / -0.9	19.8 / 19.3 / +0.5
ARC-C	LLaMA3.1-8B	16.1 / 16.1 / 0.0	11.5 / 11.5 / 0.0
	LLaMA3.2-3B	8.6 / 7.6 / +1.0	18.5 / 18.4 / +0.1
Coda-H	LLaMA3.1-8B	13.7 / 13.4 / +0.3	19.8 / 20.9 / -1.1
	LLaMA3.2-3B	8.2 / 7.5 / +0.7	19.2 / 19.9 / -0.7

Table 2: Self-consistency scores ($\times 100$) for correct (C) and incorrect (I) predictions. We denote $\Delta = C - I$. Cosine similarity and Spearman rank correlation are shown. Differences are small and vary in direction.

4 Improve Self-Consistency with DPO

To improve the self-consistency of natural language explanations, we fine-tune language models using Direct Preference Optimization (DPO) (Rafailov et al., 2023), which aligns outputs with preference signals through relative comparisons—without relying on reward models or reinforcement learning.

Preference Pair Construction. For each input \mathbf{x} , we construct preference pairs by selecting a preferred explanation $\mathbf{y}_{\text{exp}}^{\text{chosen}}$ and a dispreferred explanation $\mathbf{y}_{\text{exp}}^{\text{rejected}}$ based on their attribution alignment with the model's decision \mathbf{y}_{dec} (Section 3.2). We rank five candidate explanations using Spearman rank correlation between their attribution vectors and the decision's attribution vector, then select the highest and lowest ranked as the preference pair.

Alignment Metric. We employ Spearman rank correlation as our primary alignment metric for DPO training over the previously used cosine similarity. Spearman correlation captures feature prioritization rather than magnitude alignment. As demonstrated in Section 3.5 (Figure 3), Spearman correlation exhibits greater score variability across explanation candidates. This broader dynamic range provides a more informative training signal, enabling clearer differentiation between high-quality and low-quality explanations.

Training Procedure. To enable parameter-efficient adaptation, we apply LoRA (Low-Rank Adaptation)(Hu et al., 2021), which introduces trainable low-rank decomposition matrices into the attention and feed-forward layers of the transformer architecture. This approach allows us to adapt the model's behavior while updating only a small fraction of the total parameters, significantly reducing computational requirements and memory overhead. Throughout the training process, all explanation generations follow the same zero-shot prompting scheme detailed in Section 3.4,

Metric			LLaMA3.1-8B		LLaMA3.2-3B	
			Vanilla	Ours (↑↓)	Vanilla	Ours (↑↓)
ECQA	CC-LIME-Cos	Worst Mean Best	07.58 ± 0.11 08.05 ± 0.12 08.53 ± 0.13	07.64 ± 0.12 (↑ 0.8%) 08.10 ± 0.12 (↑ 0.6%) 08.57 ± 0.13 (↑ 0.5%)	01.11 ± 0.14 01.46 ± 0.14 01.81 ± 0.14	01.30 ± 0.13 (↑ 17.1%) 01.63 ± 0.13 (↑ 11.6%) 01.96 ± 0.13 (↑ 8.3%)
	CC-LIME-Sp	Worst Mean Best	05.00 ± 0.30 18.22 ± 0.23 31.30 ± 0.28	07.20 ± 0.30 (↑ 44%) 20.22 ± 0.23 (↑ 11%) 32.86 ± 0.29 (↑ 5%)	10.04 ± 0.31 22.52 ± 0.26 35.02 ± 0.30	$10.50 \pm 0.32 \ (\uparrow 4.6\%)$ $22.65 \pm 0.27 \ (\uparrow 0.6\%)$ $34.81 \pm 0.30 \ (\downarrow 0.6\%)$
ARC-Easy	CC-LIME-Cos	Worst Mean Best	13.32 ± 0.25 14.17 ± 0.27 15.03 ± 0.28	13.47 \pm 0.26 († 1.1%) 14.31 \pm 0.27 († 1.0%) 15.15 \pm 0.29 († 0.8%)	05.58 ± 0.32 06.13 ± 0.33 06.68 ± 0.34	05.58 ± 0.30 $06.11 \pm 0.31 (\downarrow 0.3\%)$ $06.66 \pm 0.32 (\downarrow 2.9\%)$
	CC-LIME-Sp	Worst Mean Best	-01.90 ± 0.43 12.01 ± 0.35 25.72 ± 0.43	01.84 ± 0.44 († 96.8%) 15.01 ± 0.38 († 25.0%) 28.38 ± 0.45 († 10.3%)	07.97 ± 0.45 20.72 ± 0.39 33.14 ± 0.44	$08.99 \pm 0.44 (\uparrow 12.8\%)$ $21.53 \pm 0.39 (\uparrow 3.9\%)$ $34.19 \pm 0.46 (\uparrow 3.2\%)$

Table 3: Evaluation results across tasks. Other metrics show Worst, Best, and Mean self-consistency scores across 5 explanations (×100). Each model has a vanilla and a DPO-enhanced variant.

Target Dataset	Model	Training Data	CC-Cos (↑↓)	CC-Sp (↑↓)
CODAH	LLaMA3.1-8B	None (Vanilla) ECQA (DPO-tuned) ARC-Easy (DPO-tuned)	13.50 ± 0.28 $13.39 \pm 0.27 (\downarrow 0.8\%)$ $13.38 \pm 0.27 (\downarrow 0.9\%)$	19.46 ± 0.48 $21.58 \pm 0.49 (\uparrow 10.9\%)$ $21.71 \pm 0.50 (\uparrow 11.6\%)$
	LLaMA3.2-3B	None (Vanilla) ECQA (DPO-tuned) ARC-Easy (DPO-tuned)	08.04 ± 0.34 $08.16 \pm 0.35 \ (\uparrow 1.5\%)$ $08.02 \pm 0.34 \ (\downarrow 0.2\%)$	17.95 ± 0.57 $19.41 \pm 0.54 (\uparrow 8.1\%)$ $18.13 \pm 0.57 (\uparrow 1.0\%)$
ARC-Chal	LLaMA3.1-8B	None (Vanilla) ECQA (DPO-tuned) ARC-Easy (DPO-tuned)	16.26 ± 0.33 16.48 ± 0.33 († 1.3%) 16.49 ± 0.33 († 1.4%)	11.81 ± 0.45 $13.60 \pm 0.49 \ (\uparrow 13.16\%)$ $13.87 \pm 0.49 \ (\uparrow 17.4\%)$
- 7	LLaMA3.2-3B	None (Vanilla) ECQA (DPO-tuned) ARC-Easy (DPO-tuned)	08.58 ± 0.46 08.46 ± 0.44 (↓ 1.4%) 08.49 ± 0.44 (↓ 1.0%)	19.51 ± 0.62 $19.83 \pm 0.62 (\uparrow 1.6\%)$ $19.83 \pm 0.69 (\uparrow 1.6\%)$

Table 4: Out-of-Domain Performance: Models trained on source datasets (ECQA, ARC-Easy) and evaluated on target datasets (CODAH, ARC-Challenge). Results show mean Cosine similarity (CC-Cos) and mean Spearman correlation (CC-Sp) (×100) with relative improvements over vanilla models in parentheses.

ensuring consistency between training and evaluation conditions. All models are fine-tuned independently on their respective attribution-based preference datasets. Training hyperparameters and LoRA configurations are detailed in Appendix B.

4.1 In-Domain Evaluation

Table 3 presents the results of our DPO-based approach to improving explanation self-consistency on in-domain data. We fine-tuned models on the same dataset used for evaluation to assess the direct impact of preference optimization on alignment between decisions and explanations.

LLaMA3.1-8B Performance: The DPO-tuned LLaMA3.1-8B model demonstrates substantial improvements in self-consistency across both evaluation datasets. On ECQA, while cosine similarity shows modest gains (0.5-0.8%), Spearman correlation exhibits remarkable improvement, with worst-

case scores increasing by 44% (from 5.00 to 7.20) and mean scores by 11% (from 18.22 to 20.22). Similarly, on ARC-Easy, the worst-case Spearman score jumps from -1.90 to 1.84, representing a 96.8% improvement, while mean Spearman scores increase by 25% (from 12.01 to 15.01).

LLaMA3.2-3B Performance: For the smaller LLaMA3.2-3B model, we observe mixed but generally positive results. On ECQA, cosine similarity metrics show stronger relative improvements (8.3-17.1%) compared to the larger model, though the absolute values remain lower. Spearman correlation shows more modest gains, with improvements of 0.6-4.6% across different metrics. On ARC-Easy, results are mixed, with slight decreases in cosine similarity (-0.3% for mean scores) but improvements in Spearman correlation (up to 12.8% for worst-case scores). Figure 5 shows how our model improves the consistency of the worst expla-

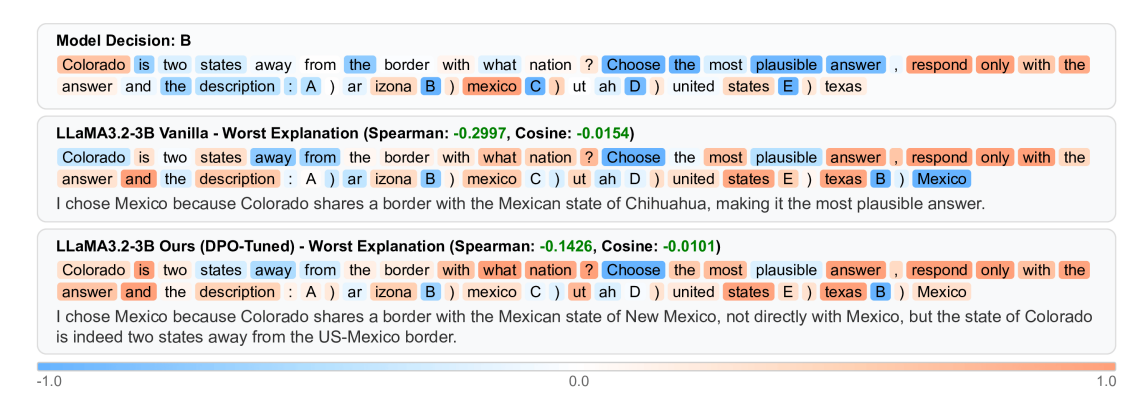


Figure 5: An example from ECQA shows attribution alignment for the LLaMA3.2-3B model's decision and its worst explanation across two variants. The model selects "B" (Mexico), with high-attribution tokens like "Colorado," "two," "states," and "Mexico" supporting its geographic reasoning. The DPO-tuned model generates a worst-case explanation that better reflects this rationale, noting Colorado's distance from Mexico, mirroring the decision attribution. In contrast, the vanilla model incorrectly references a border with "Chihuahua," unsupported by the decision attribution.

nation—not only in attribution metrics, but also in its semantic alignment with the model's decision.

Cross-Metric Transfer: Despite training exclusively with Spearman correlation as our optimization objective, we observe improvements in cosine similarity as well. This cross-metric transfer suggests that optimizing for feature rank alignment naturally enhances directional similarity between attribution vectors. The effect is particularly pronounced for LLaMA3.2-3B on ECQA, where cosine similarity improvements (8.3-17.1%) outpace Spearman correlation gains (0.6-4.6%), despite not being directly optimized. This finding indicates that prioritizing rank correlation in training has positive spillover effects on magnitude alignment, providing a more robust approach to enhancing overall self-consistency.

4.2 Cross-Domain Generalization

Table 4 reports cross-domain performance, where models trained on ECQA or ARC-Easy are evaluated on CODAH or ARC-Challenge to test generalization of self-consistency. Models fine-tuned on ECQA or ARC-Easy show consistent improvements in Spearman correlation on unseen datasets. For LLaMA3.1-8B, gains range from 10.9–17.4%, with the strongest transfer from ARC-Easy to the harder ARC-Challenge (+17.4%). The smaller LLaMA3.2-3B shows more modest but positive gains (1.0–8.1%). In contrast, cosine similarity shows minimal or slightly negative transfer. For LLaMA3.1-8B, cosine scores drop by 0.8–0.9% when transferring to CODAH, despite training on

ECQA or ARC-Easy. This reflects the distinction between rank-based and magnitude-based consistency. Notably, our models were trained using Spearman correlation only, which likely contributed to the stronger improvements in Spearman and the smaller (but occasionally positive) gains in cosine similarity, for example, a 1.4% increase from ARC-Easy to ARC-Challenge. These results suggest our DPO-based approach promotes explanation strategies that generalize beyond the training set domain, especially regarding token ranking.

5 Conclusion

We introduce PSCB, the first large-scale resource for analyzing self-consistency in natural language explanations (NLEs), spanning diverse QA datasets, instruction-tuned LLMs, and alignment metrics. Our analysis reveals key insights for improving explanation quality. Notably, we find that self-consistency is largely orthogonal to answer correctness, suggesting it captures an independent, interpretable property of model behavior. We propose Spearman rank correlation as a complementary alignment metric that better distinguishes between explanations and enables more effective optimization via DPO. Optimizing for Spearman yields substantial gains in attribution-based self-consistency that generalize across domains—without compromising cosine similarity. In fact, cosine alignment often improves despite not being optimized, indicating positive cross-metric transfer. We hope PSCB and our findings lay the groundwork for future work on developing more consistent, interpretable, and trustworthy LLMs.

Limitations

This work focuses on assessing and improving the self-consistency of natural language explanations given by LLMs. We report the following limitations:

Using only LIME. Attribution-based selfconsistency is computationally intensive: methods like CC-SHAP (Parcalabescu and Frank, 2023) take four minutes per example, making them infeasible at scale. To overcome this, we introduce CC-LIME, a more efficient variant that uses LIME (Ribeiro et al., 2016). Though still resourceheavy, CC-LIME significantly reduces runtime (about one minute per example) and scales better without relying on semantic evaluation or auxiliary models. Building the Post-hoc Consistency Bank involved attribution scoring on tens of thousands of examples from four MCQA datasets and two language models. For each of 23,290 scenarios (defined by dataset, model, and seed), we generated five explanations and computed CC-LIME for the decision and each explanation—over 139,000 attribution runs in total. This process required hundreds of GPU hours, making it one of the most extensive studies of explanation alignment to date. We also fine-tuned DPO models with attribution-based supervision and evaluated them across five seeds per model-dataset pair. While compute-intensive, this approach yields interpretable, reproducible metrics that capture a critical aspect of explanation quality—justifying the investment.

No Human Study. Self-consistency is defined as the alignment between the attribution vectors of a model's decision and its explanation. This internal property is not directly observable to human annotators and would require knowledge of how the model distributes importance across input features—something even experts lack for large models. As such, we do not employ human judgment in our evaluation. Nonetheless, assessing whether higher self-consistency also leads to more *plausible* or *helpful* explanations from a user's perspective remains an open question. Future work may explore this direction through human studies to better understand the downstream utility of self-consistency for interpretability and trust.

Model and Task Scope. We focus exclusively on small to medium scale instruction-tuned LLMs in a multiple-choice question answering (MCQA) setup.

This choice simplifies attribution computation and explanation prompting but may limit generalization to other model families (e.g., base pretrained models, encoder-decoder architectures) and open-ended tasks (e.g., summarization, reasoning chains).

Offline vs. Online. To improve the LLM's selfconsistency, we update it using DPO in an offline manner, creating a new model dedicated to providing consistent explanations. However, this approach introduces a trade-off: while the updated model generates more self-consistent explanations, it achieves only approximate self-consistency since it differs from the original model that generated the reference answers. Online learning could theoretically maintain perfect self-consistency by updating the model while continuously re-calculating attribution vectors for its own evolving outputs. Nevertheless, this approach presents significant technical challenges, including the computational overhead of recalculating attributions at each training step and potential instability in the learning dynamics, making offline training the more practical choice despite its inherent approximation.

Acknowledgments

Funded by the European Union (ERC, Convey, 101078158). Views and opinions expressed are however those of the author(s) only and do not necessarily reflect those of the European Union or the European Research Council Executive Agency. Neither the European Union nor the granting authority can be held responsible for them.

References

Shourya Aggarwal, Divyanshu Mandowara, Vishwajeet Agrawal, Dinesh Khandelwal, Parag Singla, and Dinesh Garg. 2021. Explanations for commonsenseqa: New dataset and models. In *Proceedings of the 59th Annual Meeting of the Association for Computational Linguistics and the 11th International Joint Conference on Natural Language Processing (Volume 1: Long Papers)*, pages 3050–3065.

Pepa Atanasova, Oana-Maria Camburu, Christina Lioma, Thomas Lukasiewicz, Jakob Grue Simonsen, and Isabelle Augenstein. 2023. Faithfulness tests for natural language explanations. *arXiv preprint arXiv:2305.18029*.

Sebastian Bach, Alexander Binder, Grégoire Montavon, Frederick Klauschen, Klaus-Robert Müller, and Wojciech Samek. 2015. On pixel-wise explanations for non-linear classifier decisions by layer-wise relevance propagation. *PloS one*, 10(7):e0130140.

- Michael Chen, Mike D'Arcy, Alisa Liu, Jared Fernandez, and Doug Downey. 2019. CODAH: An adversarially-authored question answering dataset for common sense. In *Proceedings of the 3rd Workshop on Evaluating Vector Space Representations for NLP*, pages 63–69, Minneapolis, USA. Association for Computational Linguistics.
- Peter Clark, Isaac Cowhey, Oren Etzioni, Tushar Khot, Ashish Sabharwal, Carissa Schoenick, and Oyvind Tafjord. 2018. Think you have solved question answering? try arc, the ai2 reasoning challenge. *arXiv* preprint arXiv:1803.05457.
- J. Edward Hu, Yelong Shen, Phillip Wallis, Zeyuan Allen-Zhu, Yuanzhi Li, Shean Wang, and Weizhu Chen. 2021. Lora: Low-rank adaptation of large language models. ArXiv, abs/2106.09685.
- Alon Jacovi and Yoav Goldberg. 2020. Towards faithfully interpretable nlp systems: How should we define and evaluate faithfulness? *arXiv preprint arXiv:2004.03685*.
- Sarthak Jain and Byron C Wallace. 2019. Attention is not explanation. *arXiv preprint arXiv:1902.10186*.
- Narine Kokhlikyan, Vivek Miglani, Miguel Martin, Edward Wang, Bilal Alsallakh, Jonathan Reynolds, Alexander Melnikov, Natalia Kliushkina, Carlos Araya, Siqi Yan, and Orion Reblitz-Richardson. 2020. Captum: A unified and generic model interpretability library for pytorch. *ArXiv*, abs/2009.07896.
- Tamera Lanham, Anna Chen, Ansh Radhakrishnan, Benoit Steiner, Carson Denison, Danny Hernandez, Dustin Li, Esin Durmus, Evan Hubinger, Jackson Kernion, and 1 others. 2023. Measuring faithfulness in chain-of-thought reasoning. *arXiv* preprint *arXiv*:2307.13702.
- Scott M Lundberg and Su-In Lee. 2017. A unified approach to interpreting model predictions. *Advances in neural information processing systems*, 30.
- Qing Lyu, Marianna Apidianaki, and Chris Callison-Burch. 2022. Towards faithful model explanation in nlp: A survey. *Computational Linguistics*, 50:657–723
- Grégoire Montavon, Alexander Binder, Sebastian Lapuschkin, Wojciech Samek, and Klaus-Robert Müller. 2019. Layer-wise relevance propagation: an overview. *Explainable AI: interpreting, explaining and visualizing deep learning*, pages 193–209.
- Sharan Narang, Colin Raffel, Katherine Lee, Adam Roberts, Noah Fiedel, and Karishma Malkan. 2020. Wt5?! training text-to-text models to explain their predictions. *arXiv preprint arXiv:2004.14546*.
- Letitia Parcalabescu and Anette Frank. 2023. On measuring faithfulness or self-consistency of natural language explanations. arXiv preprint arXiv:2311.07466.

- Vitali Petsiuk, Abir Das, and Kate Saenko. 2018. Rise: Randomized input sampling for explanation of blackbox models. *arXiv preprint arXiv:1806.07421*.
- Xin Quan, Marco Valentino, Louise A Dennis, and André Freitas. 2024. Verification and refinement of natural language explanations through llm-symbolic theorem proving. *arXiv preprint arXiv:2405.01379*.
- Rafael Rafailov, Archit Sharma, Eric Mitchell, Stefano Ermon, Christopher D. Manning, and Chelsea Finn. 2023. Direct preference optimization: Your language model is secretly a reward model. *ArXiv*, abs/2305.18290.
- Marco Tulio Ribeiro, Sameer Singh, and Carlos Guestrin. 2016. "why should i trust you?" explaining the predictions of any classifier. In *Proceedings of the 22nd ACM SIGKDD international conference on knowledge discovery and data mining*, pages 1135–1144
- Sofia Serrano and Noah A Smith. 2019. Is attention interpretable? *arXiv preprint arXiv:1906.03731*.
- Lichao Sun, Yue Huang, Haoran Wang, Siyuan Wu, Qihui Zhang, Chujie Gao, Yixin Huang, Wenhan Lyu, Yixuan Zhang, Xiner Li, and 1 others. 2024. Trustllm: Trustworthiness in large language models. arXiv preprint arXiv:2401.05561, 3.
- Mukund Sundararajan, Ankur Taly, and Qiqi Yan. 2017. Axiomatic attribution for deep networks. In *International conference on machine learning*, pages 3319–3328. PMLR.
- Hugo Touvron, Thibaut Lavril, Gautier Izacard, Xavier Martinet, Marie-Anne Lachaux, Timothée Lacroix, Baptiste Rozière, Naman Goyal, Eric Hambro, Faisal Azhar, and 1 others. 2023. Llama: Open and efficient foundation language models. *arXiv preprint arXiv:2302.13971*.
- Miles Turpin, Julian Michael, Ethan Perez, and Samuel Bowman. 2023. Language models don't always say what they think: Unfaithful explanations in chain-of-thought prompting. *Advances in Neural Information Processing Systems*, 36:74952–74965.
- Jason Wei, Xuezhi Wang, Dale Schuurmans, Maarten Bosma, Fei Xia, Ed Chi, Quoc V Le, Denny Zhou, and 1 others. 2022. Chain-of-thought prompting elicits reasoning in large language models. *Advances in neural information processing systems*, 35:24824–24837.
- Sarah Wiegreffe, Ana Marasović, and Noah A Smith. 2020. Measuring association between labels and freetext rationales. *arXiv preprint arXiv:2010.12762*.
- Sarah Wiegreffe and Yuval Pinter. 2019. Attention is not explanation. *arXiv preprint arXiv:1908.04626*.
- Haiyan Zhao, Hanjie Chen, F. Yang, Ninghao Liu, Huiqi Deng, Hengyi Cai, Shuaiqiang Wang, Dawei Yin, and Mengnan Du. 2023. Explainability for large

language models: A survey. *ACM Transactions on Intelligent Systems and Technology*, 15:1 – 38.

A Prompt Templates

Decision Prompt. To elicit the model's answer:

Question: {question text}
Choose the most plausible answer,
respond only with the answer and
the description:

- A. {option A}
- B. {option B}
- C. {option C}
- D. {option D}

Answer:

The model is expected to respond with a single letter corresponding to its chosen option and the answer content (e.g., "A. option A").

Explanation Prompt. To generate a justification for the selected answer, we prompt the model as follows:

Question: {question text}
Choose the most plausible answer,
respond only with the answer and
the description:

- A. {option A}
- B. {option B}
- C. {option C}
- D. {option D}

Selected Answer: {model's
answer}

Why did you make that choice? Explain briefly.

Explanation: {model's
explanation}

The explanation should rely only on the information provided in the question and answer choices.

B Implementation Details

Environment. All experiments were conducted using NVIDIA A100 80GB GPUs. We used Py-Torch and Hugging Face Transformers. Captum was used for attribution computations. All models were accessed through the Hugging Face Hub and run in float16 mode.

Dataset Processing. Each multiple-choice QA dataset (ECQA, ARC-Easy, ARC-Challenge, CO-DAH) was converted into a unified format consisting of the question, 4–5 answer choices, the model's predicted answer, and k=5 sampled posthoc explanations. All datasets were split into training (70%), validation (20%), and test (10%) sets using a fixed random seed (42). We precomputed attribution vectors for the model's decision and each explanation, resulting in six LIME runs per scenario.

Prompting. Decisions were elicited using the following template: "Choose the most plausible answer:", followed by the answer options. Explanations were generated using the model's answer with the prompt: "Why did you make that choice? Explain briefly." (see Appendix A for full prompt templates).

Text Generation. We used nucleus sampling with top-p=0.9, temperature = 0.7, and a maximum generation length of 400 tokens. Generation was done in a zero-shot setting. Padding tokens were manually set to a new padding token for compatibility. For each input, we generated 5 explanations using fixed random seeds ranging from 42 to 46 to ensure diversity and reproducibility.

Attribution. Feature attributions were computed using LIME with 500 perturbation samples per example, using Captum's implementation. The reference input consisted of the pad token repeated to the input length. A manually defined list of formatting and punctuation tokens was excluded from attribution (see Appendix C).

Consistency Metrics. We computed cosine similarity and Spearman rank correlation between the attribution vectors of the model's decision and each explanation. These scores were used to rank explanations and construct attribution-based preference pairs.

DPO Fine-Tuning. We used Direct Preference Optimization (DPO) to fine-tune each model using preference pairs derived from attribution alignment scores. We sampled 5 explanations per instance, ranked them using Spearman correlation, and used the highest- and lowest-ranked as the preferred and rejected explanations, respectively. Fine-tuning was done with LoRA for parameter-efficient updates. We apply LoRA with a rank of 32 and scaling factor lora_alpha = 32, targeting all

major projection layers (q_proj, k_proj, v_proj, o_proj, gate_proj, up_proj, down_proj) and disabling dropout and bias adaptation. Gradient checkpointing is enabled via the unsloth backend for memory efficiency. All models were fine-tuned independently per dataset. We summarize the hyperparameters used for fine-tuning all models in Table 5.

C Skip Tokens for Attribution

To ensure attribution focuses on semantically meaningful input content, we exclude formatting and structure-related tokens from all attribution computations. For LLaMA models, we identify a set of *skip tokens* that should not be considered when measuring input importance. These tokens include both model-specific structural markers and general-purpose formatting symbols.

Structure Tokens. Based on the tokenizer vocabulary and architecture of **LLaMA3.1** and **LLaMA3.2**, we exclude the following structure tokens when present:

- <|start_header_id|>
- <|end_header_id|>
- <|eot_id|>
- <|begin_of_text|>
- C (newline marker or formatting artifact)
- Ġ-> (common artifact from tokenizer for arrows or prompt delimiters)

These tokens typically serve as formatting scaffolding or internal delimiters in system and chat prompts, and do not reflect actual semantic content from the question or explanation.

Usage. We apply this skip list to both the decision and explanation inputs before computing attribution scores. Tokens that match the above set (by string or token ID) are held fixed during perturbation and excluded from similarity calculations between attribution vectors.

Note. We do not exclude standard stop words or punctuation in our main experiments, as their contribution may still reflect the model's learned reasoning behavior. However, our framework allows toggling this behavior for ablation studies.

D Qualitative Examples Heatmaps

Figure 6 presents token-level attribution heatmaps for model decisions and explanations, using the LIME method. Each subfigure illustrates a different scenario from the ECOA dataset, comparing the best and worst explanations produced by vanilla models based on Spearman and Cosine alignment scores. Across examples, we observe that highquality explanations (left) tend to emphasize tokens that align more closely with the model's decision rationale—for instance, highlighting locationspecific cues like "eastern coast" or situational context like "board room." In contrast, low-ranking explanations (right) often shift focus to semantically irrelevant or misleading tokens, despite sounding plausible. These visualizations underscore the discriminative power of attribution-based metrics and highlight the variability in explanation quality for the same input.

Hyperparameter	ECQA (L3.1)	ARC-Easy (L3.1)	ECQA (L3.2)	ARC-Easy (L3.2)
Epochs	10	10	10	10
Batch Size	16	16	16	16
Gradient Accumulation	8	8	8	8
Learning Rate	4.21×10^{-6}	4.65×10^{-6}	9.55×10^{-6}	6.32×10^{-6}
DPO Beta	5.13	5.64	8.44	8.84
Score Scale Factor	10	10	10	10
Optimizer	AdamW	AdamW	AdamW	AdamW

Table 5: Hyperparameters used for DPO fine-tuning across model-dataset pairs.



Figure 6: Qualitative heatmap visualizations showing token-level attribution scores for model decisions and explanations using the LIME method.